Published in final edited form as:
Exp Cell Res. 2007 April 15; 313(7): 1473–1483.

Zinc transporter 2 (SLC30A2) can suppress the vesicular zinc defect of adaptor protein 3-depleted fibroblasts by promoting zinc accumulation in lysosomes

Juan M. Falcón-Pérez* and **Esteban C. Dell'Angelica**
Department of Human Genetics, David Geffen School of Medicine, University of California, Los Angeles, CA 90095, USA

Abstract

Zinc accumulation in the lumen of cytoplasmic vesicles is one of the mechanisms by which cells can store significant amounts of this essential but potentially toxic biometal. Previous studies had demonstrated reduced vesicular zinc levels in fibroblasts from mutant mice deficient in adaptor protein 3 (AP-3), a complex involved in protein trafficking to late endosomes and lysosomes. We have observed a similar phenotype in the human fibroblastoid cell line, M1, upon small interference RNA-mediated AP-3 knockdown. A survey of the expression and localization of zinc transporter (ZnT) family members identified ZnT2, ZnT3 and ZnT4 as likely mediators of vesicular zinc accumulation in M1 cells. Expression of green fluorescence protein (GFP)-tagged ZnT2 and ZnT3 promoted accumulation of vesicular zinc as visualized using the indicator zinquin. Moreover, GFP-ZnT2 overexpression elicited a significant accumulation of zinc within mature lysosomes, which in untransfected M1 cells contained little or no chelatable zinc, and restored the zinc storage capability of AP-3-deficient cells. These results suggest that ZnT2 can facilitate vesicular zinc accumulation independently of AP-3 function, and validate the M1 fibroblastoid line as a human cell culture system amenable to the study of vesicular zinc regulation using techniques compatible with functional genomic approaches.

Keywords

AP-3; Hermansky-Pudlak Syndrome; SLC30A; zinc transporter; Zinquin; ZnT

Introduction

Zinc is an essential trace element for all living organisms and is required for a wide range of biological processes, including DNA and RNA synthesis as well as protein stability and activity (reviewed in Refs. [1,2]). In humans, zinc deficiency has been associated with dermatitis, growth retardation, poor wound healing, and impaired immune, mental and reproductive functions [1-4]. At the cellular level, zinc is essential for cell proliferation and differentiation [4,5]. However, high levels of zinc can be cytotoxic [6,7]. In mammalian cells, very little zinc exists in free form in the cytosol [8]. Rather, it is stored in at least three pools: tightly bound to a wide variety of proteins, bound to metallothioneins, and accumulated in the lumen of

*Corresponding author. Present address: CIC bioGUNE, Technological Park of Bizkaia, Bldg. 801-A, 48160 DERIO, Spain. Phone: 34-944-061-319 Fax: 34-944-061-301 Email: jfalcon@cicbiogune.es

cytoplasmic vesicles or organelles [1,8]. This third pool, which has occasionally been called "the zincosome" [5] and is herein referred to as "vesicular zinc" or "chelatable zinc stores," corresponds to zinc in a form that can be readily chelated by permeable Zn(II) fluorophore sensors such as zinquin [9-11].

Transport of zinc across the plasma membrane and the limiting membranes of intracellular organelles is mediated by two separate families of integral membrane proteins: the Zrt- and Irt-like proteins (ZIP), also known as solute-linked carrier 39A (SLC39A) family members, and the zinc transporter (ZnT)/cation diffusion facilitator/SLC30 family members [8,12]. The ZIPs facilitate zinc uptake into the cytosol from the extracellular milleu or transport out of the lumenal compartment of cytoplasmic vesicles and organelles. Conversely, most ZnT family members facilitate removal of zinc from the cytosol, either out of the cell or into the lumen of vesicles and organelles [8,12,13]. Ten genes encoding ZnT protein family members (ZnT1 through ZnT10, or SLC30A1 through SLC30A10) have been identified in the human genome [14]. ZnT9 (SLC30A9, also known as HUEL or C4orf1) is the most divergent member of the family and may not function in zinc transport but rather in DNA excision-repair [15,16]. The ZnT10 protein has not yet been characterized, thus its role in zinc transport remains hypothetical [14]. For ZnT1 through ZnT8, compelling evidence supports a role in zinc transport. For instance, ZnT1 is ubiquitously expressed and targeted to the plasma membrane, where it mediates zinc efflux from the cell [17], and its elimination by targeted disruption of the *Znt1* gene in mice has been reported to result in embryonic lethality [13]. ZnT3 is expressed mostly in brain, where it localizes to zinc-containing synaptic vesicles within a subset of glutamatergic neurons [18-20]. Knockout mice lacking ZnT3 are viable but display a severe depletion of zinc in synaptic vesicles [21]. ZnT4 is expressed ubiquitously [22,23] and localized to cytoplasmic organelles [24,25], although its exact subcellular distribution remains unsettled. Mice of the lethal milk (*lm*) strain carry a nonsense mutation in *Znt4* [22]; the milk of these mice is depleted of zinc and do not support the normal development of pups. ZnT5 is also expressed ubiquitously, has been localized to the Golgi apparatus and insulin-containing granules [26,27], and its elimination by targeted disruption of the *Znt5* gene in mice has been shown to result in osteopenia and sudden cardiac death [27]. Finally, ZnT2, ZnT6, ZnT7 and ZnT8 have all been localized to intracellular compartments and all but ZnT8 seem to be expressed in a wide variety of cell types [10,13,14,25,28,29].

Our interest in the regulation of vesicular zinc stores within mammalian cells stems from our studies on adaptor protein-3 (AP-3), a heterotetrameric protein complex involved in the sorting of integral membrane proteins within the endosomal/lysosomal system [30]. Two forms of AP-3 have been characterized: a ubiquitous form, containing the δ, β3A, μ3A and σ3(A/B) subunits, and a brain-specific form, containing β3B and μ3B in addition to the common δ and σ3(A/B) subunits [30]. Mutations in the human *AP3B1* gene encoding the β3A subunit of ubiquitous AP-3 result in Hermansky-Pudlak syndrome (HPS) type 2, an autosomal recessive disorder in which oculocutaneous albinism, bleeding, and other manifestations result from defects in multiple lysosome-related organelles, including melanosomes and platelet-dense granules [31]. A comparable phenotype is observed in pearl mice, which carry mutations in *Ap3b1* [32], or in knockout mice generated by targeted disruption of the same gene [33]. Interestingly, the mocha mice, which carry mutations in the gene encoding the δ subunit common to both the ubiquitous and brain-specific forms of AP-3, display not only the HPS-like phenotype but also abnormal behavior and severe reductions in synaptic vesicle zinc and ZnT3 immunoreactivity within the hippocampal mossy fibers [34]. Subsequent studies have reinforced the idea that ZnT3 trafficking and synaptic vesicle zinc are controlled by the brain-specific form of AP-3, as demonstrated both *in vitro* [35] and in mice lacking the brain-specific β3B subunit [36]. Importantly, evidence has also been obtained for a role of the ubiquitous AP-3 form in regulating chelatable zinc stores. Thus, immortalized skin fibroblasts derived from *Ap3b1* knockout mice [33] and the pearl [37,38] and mocha [39] mutant mice all displayed

significantly reduced zinquin fluorescence associated with cytoplasmic foci, as compared to control fibroblasts from wild-type mice. Although the exact mechanism by which AP-3 influences chelatable zinc stores in fibroblasts remains unclear, it seems reasonable to speculate that AP-3 might regulate the trafficking of one or more ZnT family members to late endosomes and/or lysosomes, where zinc is thought to be stored [10,40]. However, the functional relationships between AP-3 and ZnT family members in cells of non-neuronal origin (*e.g.*, fibroblasts) have not been examined.

In this work, we have used the human fibroblastoid cell line, M1, to investigate potential functional interactions between AP-3 and ZnT family members and their effects on vesicular zinc stores. Besides being the cell line in which the ubiquitous form of AP-3 was first characterized [41], M1 cells grow well on glass and plastic surfaces under standard culture conditions and are easy to manipulate by transient and stable transfection as well as by small interference RNA (siRNA), thus making this cell line amenable to functional genomic approaches. We herein report that most ZnT family members are expressed in M1 cells, that three of them are targeted to lysosome-associated membrane protein 1 (LAMP1)-positive late endosomes and lysosomes, and that overexpression of one of them - ZnT2 - can restore the zinc storage capability of AP-3-deficient cells by promoting zinc accumulation in mature lysosomes.

Materials and methods

Cell culture

The sources and culture conditions of the human cell lines M1, HeLa and MNT-1 have been described previously [42].

Transcript expression analysis

Total RNA was isolated using the TRIzol Reagent (Invitrogen, Carlsbad, CA, USA) as per the manufacturer′s instructions. The expression of human ZnT1 (SLC30A1; GenBank accession no. **NM_021194**), ZnT2 (SLC30A2; GenBank accession no. **NM_001004434**), ZnT3 (SLC30A3; GenBank accession no. **NM_003459**), ZnT4 (SLC30A4; GenBank accession no. **NM_013309**), ZnT5 (SLC30A5; GenBank accession no. **NM_022902**), ZnT6 (SLC30A6; GenBank accession no. **NM_017964**), ZnT7 (SLC30A7; GenBank accession no. **NM_133496**), ZnT8 (SLC30A8; GenBank accession no. **NM_173851**) and ZnT10 (SLC30A10; GenBank accession no. **NM_018713**) was examined by reverse transcriptase-polymerase chain reaction (RT-PCR) using SuperScript one-step RT-PCR system with Platinum Taq DNA polymerase (Invitrogen, Carlsbad CA, USA) in a PTC-100 thermal cycler (MJ Research, Waltham, MA, USA). The specific primers (and expected product sizes, in base pairs) were: 5′-gtc aac gtg ctg ggg ctc tgc and 5′-cta caa tca ctg aac cca agg for ZnT1 (412 bp), 5′-gct tgg ctg tca tga ctg acg and 5′-tct acc ccc tcc acc gac agc for ZnT2 (613 bp), 5′-acg tgc tgg ggg acc tcc tgc and 5′-ctg tga tca ggg cag cag atg for ZnT3 (532 bp), 5′-gtc agc tga gtt tga agg tgg and 5′-gtg agt atg atg gcg ctt agg for ZnT4 (214 bp), 5′-gac atg agg aga ccc cgc gac and 5′-gag tga aat aat aca ccc agc for ZnT5 (374 bp), 5′-ctt act cca gac aac acc acc and 5′-taa aca gtc aat gca aag ttg for ZnT6 (708 bp), 5′-gga gta gac ccg gcc ctt cgc and 5′-aca aga agc agt ctc tca tgg for ZnT7 (464 bp), 5′-tga tta cca gat cca ggc gac and 5′-gca tag cag cat gtt tga agg for ZnT8 (663 bp), 5′-tgc ttc ccc tga aga gtg agg and 5′-aag ttc cca gat gtg cac ttc for ZnT10 (224 bp). The RT-PCR products were analyzed by 2.5% (w/v) agarose gel electrophoresis in the presence of ethidium bromide, and photographed under ultraviolet light with a digital camera. The identity of the RT-PCR products was verified by gel purification followed by direct DNA sequencing.

DNA constructs

To generate expression plasmids coding the human proteins ZnT1, ZnT2, ZnT3, ZnT4, ZnT5, ZnT6, ZnT7 and CD63 fused to green fluorescence protein (GFP) or to the myc epitope, the complete open-reading frames of ZnT1 (SLC30A1; RefSeq accession no. **NP_067017**), ZnT2 (SLC30A2; RefSeq accession no. **NP_001004434**), ZnT3 (SLC30A3; RefSeq accession no. **NP_003450**), ZnT4 (SLC30A4; RefSeq accession no. **NP_037441**), ZnT5 (SLC30A5; RefSeq accession no. **NP_075053**), ZnT6 (SLC30A6; RefSeq accession no. **NP_060434**), ZnT7 (SLC30A7; RefSeq accession no. NP_598003) and CD63 (RefSeq accession no. **NP_001771**) were amplified by PCR from Marathon-Ready cDNA derived from human HeLa S3 cells (BD Biosciences Clontech, Mountain View, CA, USA). The products were purified and used as templates for nested PCR, using primers designed to append an *Eco*RI site upstream of the Kozak sequence and to replace the translation termination site by a *Sal*I site, followed by myc-coding sequence, a stop codon and a *Not*I site. The nested PCR product was gel-purified and cloned in the *Eco*RI-*Sal*I sites of the pEGFP-C2 and pEGFP-N3 vectors (BD Biosciences Clontech, Mountain View, CA, USA) for expression of GFP-tagged proteins, or in the *Eco*RI-*Not*I of the pCR3.1 vector (Invitrogen, Carlsbad, CA, USA) for expression of myc-tagged proteins. All constructs were verified by DNA sequencing.

Transient transfection with expression plasmids and generation of stably transfected cell lines

For transient expression of GFP- or myc-tagged Znt proteins, M1 cells grown on twelve-well plates were transfected with 1 μg/well of purified expression plasmid using the FuGENE 6 reagent (Roche Molecular Biochemicals, Indianapolis, IN, USA) according to the manufacturer's instructions. Cells were analyzed 24 h after transfection. For stable expression, cells were grown at 37°C in complete DMEM [DMEM supplemented with 10% (v/v) fetal bovine serum, 2 mM glutamine, 0.1 mg/ml streptomycin, and 100 units/ml penicillin] to 60-70% confluency and transfected with expression plasmids encoding GFP-ZnT2, GFP-ZnT3, GFP-ZnT4, ZnT2-GFP, ZnT3-GFP, ZnT4-GFP or CD63-GFP fusion proteins, using FuGENE 6 in serum-free DMEM. The medium was changed five hours after transfection to complete DMEM, and one day later to complete DMEM containing 2 mg/ml G418. About two weeks later, Clones of stably transfected cells were isolated by limiting dilution and maintained in complete DMEM containing 2 mg/ml G418.

Knockdown of AP-3 expression by siRNA

M1 fibroblasts were seeded at a density of $3x10^5$ cells per 9-cm dish and cultured for at least 12 h. Treatment with siRNA duplexes was performed as follows: for each 9-cm dish, 25 μl of OligofectAMINE ((Invitrogen, Carlsbad, CA, USA) was added to 100 μl Opti-MEM I (Invitrogen, Carlsbad, CA, USA) and the mixture was incubated for 5-10 min at room temperature prior to its transfer to a tube containing 800 μl of Opti-MEM I and 50 μl of 20 μM siRNA and further incubation for 15-20 min at room temperature. Subsequently, Opti-MEM I was added to final volume of 5 ml, and the final mixture was added to the cell monolayer previously rinsed once with Opti-MEM I. Following a 4-h incubation at 37°C, 5 ml of DMEM containing 20% (v/v) fetal bovine serum and 2 mM glutamine (no antibiotics) were added, and the cells were left in this mixture until the following day, when they were trypsinized and seeded into two 9-cm dishes per original dish. Two days later, a second transfection was performed as described above, and the following day trypsinized again and seeded in 9-cm dishes containing glass coverlips. For AP-3 protein complex knockdown, the target was the δ subunit of the complex. The AP3D1 siRNA target sequence was: gcg aga aac ugc cua uuc a. Scrambled sequence (cga uga gaa cga uca aga aga), which had no homology to any mammalian mRNA, was used as a control siRNA. Both sense and antisense strands were synthesized as

Option A4 siRNAs by Dharmacon Research Inc (Lafayette, PA, USA). The extent of AP-3 knockdown was estimated by immunoblotting analysis of whole-cell lysates prepared directly in sample buffer for gel electrophoresis [41], using the β3A1 rabbit polyclonal antibody against the β3A subunit of AP-3 [43] or commercial mouse monoclonal antibodies against the μ3A subunit of AP-3 (BD Pharmingen, San Diego, CA, USA) and α-tubulin and β-actin (Sigma-Aldrich, St. Louis, MO, USA).

Labelling of lysosomes with Texas-red-conjugated dextran

Cells were incubated at 37°C in complete DMEM containing 0.125 mg/ml of Texas red-conjugated fixable dextran (Molecular Probes, Eugene, OR, USA). After 16 hours, the cells were trypsinized, plated onto dishes containing glass coverslips, and incubated for a 12-h chase period in complete DMEM medium lacking dextran.

Zinquin staining

Cells were incubated with 50 μM $ZnSO_4$ in calcium/magnesium-free Hanks' balanced salt solution containing 10 mM sodium pyruvate, 10 mM glucose, 100 units/ml penicillin, and 100 μg/ml streptomycin, for 1 h at 37°C. Cells were washed once and then incubated with 50 μM zinquin ethyl ester (Toronto Research Chemicals, Canada) in 10 mM glucose prepared in Dulbecco's phosphate-buffered saline (D-PBS), for 20 min at 37°C. Excess dye was removed by extensive washes. Cells were fixed in PBS containing 4% (w/v) paraformaldehyde for 10 min at room temperature, and then visualized directly by two-photon laser scanning microscopy.

Immunofluorescence staining

Mouse monoclonal antibody H4A3 to human LAMP1 was purchased from the Development Studies Hybridoma Bank (Iowa City, IA, USA). Fixed cells were first incubated for 1 h with primary antibody diluted in PBS containing 0.1% (w/v) saponin and 0.1% (w/v) bovine serum albumin, washed in PBS, and then incubated for 30 min with Cy3-conjugated donkey anti-mouse IgG (Jackson ImmunoResearch, West Grove, PA, USA) diluted in the same buffer. Stained samples were washed extensively with PBS and mounted on glass slides using Fluoromount-G (Southern Biotechnology Associates, Birmingham, AL, USA).

Confocal and two-photon laser scanning microscopy

Fluorescent samples were examined on a Leica TCS SP multiphoton confocal microscope (Leica, Germany). Zinquin was excited with a two-photon laser (Ti:sapphire) tuned at 770 nm. Images from GFP, Cy3 or Texas-Red and zinquin fluorescence were acquired using a Plan Apochromat 63x/1.4 oil objective and the Leica Confocal Software. Control experiments corroborated the lack of significant "bleed through" between the different fluorescence channels used in this study. Image analysis of randomly selected cells was carried out using the NIH Image v1.62 software.

Flow Cytometry

Cells were incubated in 50 μM $ZnSO_4$ for 1 h at 37°C, washed to remove extracellular zinc, and incubated with 50 μM zinquin ethyl ester as described above. Excess dye was extensively washed with ice-cold, calcium- and magnesium-free PBS. Subsequently, cells were lifted with PBS containing 20 mM EDTA, passed through a 100 μm cell strainer (Millipore, Bedford, MA, USA) and fixed in PBS containing 4% (w/v) paraformaldehyde for 10 min at room temperature. Cells were washed once with PBS containing 25 mM glycine and two times with PBS lacking glycine, and finally suspended in 1 ml of PBS. Zinquin and GFP fluorescence were determined in a BD-LSR I flow cytometer (Becton Dickinson, San Jose, CA, USA). The

laser used for the forward and side scatter and GFP excitation was a 488-nm argon laser. Zinquin was excited with a heliumcadmium laser set to 325 nm. Data analysis was performed using CellQuest.

Results and discussion

Vesicular zinc stores in human M1 cells

We first examined the intracellular pools of chelatable zinc in human M1 fibroblasts using zinquin, a highly specific zinc-chelating fluorescent probe that has been used to detect pools of labile Zn(II) in several cells and tissues (for example, see Refs. [9,10,33,44,45]). M1 fibroblasts grown on glass coverslips under standard cell culture conditions were incubated with zinquin and examined by two-photon laser scanning microscopy (see *Materials and methods*), resulting in detection of a discrete number of fluorescent foci representing accumulation of chelatable zinc in cytoplasmic vesicles/organelles (Fig. 1a). When cells were incubated with 50 μM $ZnSO_4$ prior to zinquin loading, both the number and relative fluorescence intensity of zinquin associated with zinc-positive compartments increased dramatically (Fig. 1b), suggesting that, as described for other mammalian cell lines [10,28, 29,45], cultured M1 cells are capable of storing excess zinc into the lumen of intracellular organelles. As expected, under identical microscopic and image processing conditions no significant fluorescence signal was detected in cells that had been incubated with $ZnSO_4$ but not with zinquin (Fig. 1c). For consistency, subsequent experiments were carried out using M1 cells that had been incubated with $ZnSO_4$prior to zinquin loading.

Expression and intracellular distribution of ZnT family members in M1 cells

We next sought to determine which members of the ZnT family (SLC30A) of putative zinc transporters are expressed in M1 cells. As mentioned above in the *Introduction* section, ten members of this family have been described in humans, and most of them have been implicated in the transport of zinc out of the cytosol, either to the extracellular space (*e.g.*, ZnT1) or into the lumen of cytoplasmic organelles (reviewed in Refs. [8,12,13]). The expression of transcripts encoding all ZnT family members other than ZnT9 (which has been implicated in DNA excision-repair [15,16]) was examined by RT-PCR. As shown in Fig. 1d, M1 cells expressed transcripts for ZnT1 through ZnT8. No expression of ZnT10 was detected in M1 cells, while the corresponding transcript was amplified from RNA isolated from HeLa cells (Table 1).

Next, we examined the subcellular distribution of ZnT1 through ZnT7 expressed as epitope-tagged proteins by transfection in M1 cells (technical difficulties encountered during isolation of a full-length ZnT8 cDNA hampered our analysis of the subcellular distribution of ZnT8). Because the type and position of the epitope tag might affect intracellular targeting, cells expressing fusion constructs bearing GFP and myc tags, at either amino- or carboxyl-termini, were analyzed. Bearing in mind that high levels of protein overexpression can also affect localization, for each tagged construct those cells expressing the highest levels (as inferred from their fluorescence signal) were excluded from the analysis. The results are listed in Table 1. All tagged forms of ZnT1 localized primarily to the plasma membrane. In contrast, ZnT5 and ZnT6 were exclusively localized at the Golgi complex, and ZnT7 was predominately associated with the Golgi complex as well as some peripheral vesicular structures. These results are essentially consistent with published data on the localization of these four ZnT family members in other cell types [17,25,27,28], although localization to vesicular structures has also been described for ZnT5 expressed in pancreatic beta-cells [26]. Out of the seven ZnT family members analyzed, ZnT2, ZnT3 and ZnT4 displayed punctuate distribution patterns that were

similar to that of chelatable zinc stores in M1 cells (Table 1). Consequently, subsequent analyses were focused on these three ZnT family members.

To address the localization of ZnT2, ZnT3 and ZnT4 in more detail, stable cell lines expressing GFP-tagged forms of these proteins were derived from the parental M1 line, and the intracellular patterns of GFP fluorescence were compared to those resulting from immunostaining using antibodies to specific organelle markers. As shown in Fig. 2, extensive colocalization was observed between each of ZnT2, ZnT3 and ZnT4, and LAMP1, which is a well known marker of late endocytic organelles (*i.e.*, late endosomes and lysosomes). In contrast, we observed minimal colocalization between any of these ZnT family members and markers of early and/or recycling endosomes (*i.e.*, early endosomal antigen 1 and transferrin receptor; data not shown). The localization of ZnT2 to LAMP1-positive compartments was consistent with a previous report on the localization of rat ZnT2 to acidic compartments within BHK cells [10]. Therefore, these results suggest that ZnT2, ZnT3 and ZnT4 are targeted to late endocytic organelles within M1 cells.

Expression of ZnT2 or ZnT3 can enhance accumulation of chelatable zinc in cytoplasmic vesicles of M1 cells

We next sought to examine the degree of colocalization between GFP-tagged ZnT2, ZnT3 and ZnT4 and vesicular zinc stores. During the course of these experiments, we noticed that cells expressing GFP-ZnT2 consistently displayed increased zinquin fluorescence signal, a phenomenon that had been previously noted in ZnT2-overexpressing BHK cells [10,40]. To address this issue in more detail, M1 cells stably expressing GFP-ZnT2 were cocultured with parental M1 fibroblasts that had been pre-loaded with Texas-red-conjugated dextran (to unambiguously identify GFP-ZnT2-negative cells on the basis of their Texas-red fluorescence signal), and the mixed cell population was incubated with $ZnSO_4$ and subsequently loaded with zinquin to detect intracellular stores of chelatable zinc. As exemplified by the images shown in Fig. 3a-c, the overall intensity of zinquin staining was higher in GFP-ZnT2-expressing cells than in GFP-ZnT2-negative, Texas-red-dextran-positive M1 cells (unpaired two-tail Student's *t*-test: $p<0.001$). This phenomenon was not due to a "bleed through" of GFP fluorescence signal into the zinquin fluorescence channel, as inferred from control experiments in which other GFP-tagged proteins expressed at comparable levels (as judged from GFP fluorescence intensity) were unable to elicit a similar effect (Fig. 3d-f and data not shown). To verify these results by an alternative method, and to extend the analysis to other ZnT family members, M1 cells expressing ZnT2, ZnT3 and ZnT4 tagged with GFP at their amino-termini (GFP-ZnT2, GFP-ZnT3 and GFP-ZnT4) or carboxyl-termini (ZnT2-GFP, ZnT3-GFP and ZnT4-GFP) were loaded with zinquin and analyzed by flow cytometry. Both GFP and zinquin fluorescence signals were measured for each cell, and the zinquin fluorescence intensity values of those cells expressing high levels of each GFP-fusion protein were compared to those of cells expressing comparable levels of an irrelevant GFP-fusion protein (*i.e.*, the same "gate" of GFP fluorescence values was used to analyze all samples). As shown in Fig. 3g, M1 cells expressing GFP-ZnT2 displayed a distribution of zinquin fluorescence with a median about five-fold higher than that of control cells. M1 cells expressing ZnT3-GFP also displayed increased zinquin fluorescence relative to control cells, although the effect was less dramatic (~2 fold); this result is at variance with previous studies in which overexpression of ZnT3 failed to promote accumulation of chelatable zinc in BHK [18] or PC12 [46,47] cells. The relative position of the GFP moiety influenced the ability of ZnT2 and ZnT3 to promote vesicular zinc accumulation. Thus, the median zinquin fluorescence of cells overexpressing ZnT2-GFP (*i.e.*, with GFP fused at the carboxyl terminus of ZnT2) or GFP-ZnT3 (*i.e.*, with GFP fused at the amino terminus of ZnT3) was only moderately increased (<60%) relative to control cells (Fig. 3g). Neither ZnT4 construct was able to elicit any significantly increase in

zinquin staining upon overexpression (Fig. 3g). Therefore, overexpression of GFP-ZnT2 and, to a lesser extent, ZnT3-GFP was able to enhance vesicular zinc accumulation in M1 cells.

As exemplified by the representative images shown in Fig. 4a-c, the GFP fluorescence signal of GFP-ZnT2-expressing cells overlapped extensively with the zinquin fluorescence signal. However, we also observed that the degree of colocalization between the GFP and zinquin fluorescence signals was relatively lower in cells expressing ZnT2-GFP, GFP-ZnT3 or either GFP-ZnT4 or ZnT4-GFP (Fig. 4d-l and data not shown), despite significant localization of all of these GFP-fusion proteins to LAMP1-positive late endocytic organelles (Fig. 2 and data not shown). These results prompted us to test whether overexpression of GFP-ZnT2 elicited a shift in the distribution of vesicular zinc, for instance by promoting sequestration of zinc in organelles that normally do not accumulate significant amounts of this biometal. To address this question, cells were loaded with Texas-red-conjugated dextran under conditions in which lysosomes were specifically labeled (*i.e.*, long chase periods to allow trafficking of all endocytosed dextran to lysosomes), subjected to transient transfection with the GFP-ZnT2-encoding plasmid (to obtain a mixture of GFP-ZnT2-expressing and GFP-ZnT2-negative cells), and subsequently incubated with $ZnSO_4$ and zinquin to label chelatable zinc stores. As exemplified by the images shown in Fig. 5, the degree of colocalization between zinquin and Texas-red fluorescence signals was dramatically higher in GFP-ZnT2-positive cells than in GFP-ZnT2-negative cells, indicating that overexpression of GFP-ZnT2 elicited a change in the subcellular distribution of chelatable zinc by promoting its sequestration into the lumen of mature lysosomes.

Overexpression of ZnT2 suppresses the defect in vesicular zinc stores caused by knockdown of AP-3 in M1 cells

As mentioned above in the *Introduction* section, immortalized skin fibroblasts derived from mice deficient in the AP-3 protein complex have been shown to display significantly reduced pools of vesicular zinc [33,37-39]. To explore this AP-3-related phenotype in human M1 fibroblasts, cells were treated with a siRNA duplex designed to specifically target the mRNA encoding the δ subunit of AP-3 or, as a control, an irrelevant siRNA duplex. As shown in Fig. 6a, targeting of the AP-3 δ subunit effectively depleted the endogenous AP-3 complex (see also Ref. [48]). M1 cells depleted of AP-3 displayed a significant reduction in zinquin fluorescence relative to control siRNA-treated cells (Fig. 6c). On the other hand, the steady-state distributions of ZnT2, ZnT3 or ZnT4 were not noticeably affected (data not shown). To determine whether overexpression of ZnT2 or ZnT3 could suppress the vesicular zinc defect of AP-3-depleted cells, siRNA-treated M1 fibroblasts were transfected with plasmids encoding GFP-ZnT2 or ZnT3-GFP, incubated with $ZnSO_4$ and zinquin, and examined by two-photon laser scanning microscopy. As shown in Fig. 6c, overexpression of GFP-ZnT2 restored the zinquin fluorescence level of AP-3-depleted cells to almost that of control cells. Again, this effect was not due to a "bleed through" of GFP fluorescence signal into the zinquin fluorescence channel, as overexpression of ZnT3-GFP to levels comparable to those of GFP-ZnT2 (as judged from GFP fluorescence; see Fig. 6b) failed to increase the zinquin fluorescence signal of AP-3-depleted cells (Fig. 6c). Taken together, these results suggest that ZnT2 can bypass the requirement for AP-3 in protein trafficking to late endosomes and lysosomes and facilitate zinc accumulation in these organelles. Alternative protein trafficking pathways to these organelles are known to exist [30] and might be used by ZnT2, at least when expressed at high levels.

In summary, we have shown that human M1 fibroblasts contain chelatable zinc stores that can be influenced by perturbations in the functions of the AP-3 complex, ZnT2 and, to a lesser extent, ZnT3. The fact that M1 cells are amenable to effective siRNA knockdown as well as

to transient and stable transfection with high efficiency makes them suitable for future studies on vesicular zinc regulation using a functional genomics approach.

Acknowledgments

We thank Drs. Cristina A. Ghiani and David E. Krantz for critical reading of the manuscript. This work was supported in part by grant HL068117 from the NIH (to E.C.D.'A.).

Abbreviations:

AP-3, adaptor protein-3; bp, base pair; GFP, green fluorescence protein; HPS, Hermansky-Pudlak syndrome; LAMP, lysosome-associated membrane protein; PBS, phosphate-buffered saline; PCR, polymerase chain reaction; RT-PCR, reverse transcriptase-PCR; siRNA, small interference RNA; SLC, solute-linked carrier; ZIP, Zrt- and Irt-like protein; ZnT, zinc transporter..

References

[1]. Maret W. Zinc biochemistry, physiology and homeostasis - recent insights and current trends. Biometals 2001;14:187–190.

[2]. Walker CF, Black RE. Zinc and the risk for infectious disease. Annu. Rev. Nutr 2004;24:255–275. [PubMed: 15189121]

[3]. Hambidge M. Human zinc deficiency. J. Nutr 2000;130:1344S–1349S. [PubMed: 10801941]

[4]. Bohnsack BL, Hirschi KK. Nutrient regulation of cell cycle progression. Annu Rev. Nutr 2004;24:433–453. [PubMed: 15189127]

[5]. Beyersmann D, Haase H. Functions of zinc in signaling, proliferation and differentiation of mammalian cells. Biometals 2001;14:331–341. [PubMed: 11831463]

[6]. Koh JY, Suh SW, Gwag BJ, He YY, Hsu CY, Choi DW. The role of zinc in selective neuronal death after transient global cerebral ischemia. Science 1996;272:1013–1016. [PubMed: 8638123]

[7]. Capasso M, Jeng JM, Malavolta M, Mocchegiani E, Sensi SL. Zinc dyshomeostasis: a key modulator of neuronal injury. J. Alzheimers Dis 2005;8:93–108. [PubMed: 16308478]

[8]. Kambe T, Yamaguchi-Iwai Y, Sasaki R, Nagao M. Overview of mammalian zinc transporters. Cell. Mol. Life Sci 2004;61:49–68. [PubMed: 14704853]

[9]. Zalewski PD, Forbes IJ, Betts WH. Correlation of apoptosis with change in intracellular labile Zn (II) using zinquin [(2-methyl-8-p-toluenesulphonamido-6-quinolyloxy)acetic acid], a new specific fluorescent probe for Zn(II). Biochem. J 1993;296:403–408. [PubMed: 8257431]

[10]. Palmiter RD, Cole TB, Findley SD. ZnT-2, a mammalian protein that confers resistance to zinc by facilitating vesicular sequestration. EMBO J 1996;15:1784–1791. [PubMed: 8617223]

[11]. Kimura E, Aoki S. Chemistry of zinc(II) fluorophore sensors. Biometals 2001;14:191–204. [PubMed: 11831456]

[12]. Liuzzi JP, Cousins RJ. Mammalian zinc transporters. Annu. Rev. Nutr 2004;24:151–172. [PubMed: 15189117]

[13]. Palmiter RD, Huang L. Efflux and compartmentalization of zinc by members of the SLC30 family of solute carriers. Pflugers Arch 2004;447:744–751. [PubMed: 12748859]

[14]. Seve M, Chimienti F, Devergnas S, Favier A. In silico identification and expression of SLC30 family genes: an expressed sequence tag data mining strategy for the characterization of zinc transporters' tissue expression. BMC Genomics 2004;5:32–41. [PubMed: 15154973]

[15]. Sim DL, Chow VT. The novel human HUEL (C4orf1) gene maps to chromosome 4p12-p13 and encodes a nuclear protein containing the nuclear receptor interaction motif. Genomics 1999;59:224–233. [PubMed: 10409434]

[16]. Sim del LC, Yeo WM, Chow VT. The novel human HUEL (C4orf1) protein shares homology with the DNA-binding domain of the XPA DNA repair protein and displays nuclear translocation in a cell cycle-dependent manner. Int. J. Biochem. Cell Biol 2002;34:487–504. [PubMed: 11906820]

[17]. Palmiter RD, Findley SD. Cloning and functional characterization of a mammalian zinc transporter that confers resistance to zinc. EMBO J 1995;14:639–649. [PubMed: 7882967]

[18]. Palmiter RD, Cole TB, Quaife CJ, Findley SD. ZnT-3, a putative transporter of zinc into synaptic vesicles. Proc. Natl. Acad. Sci. U. S. A 1996;93:14934–14939. [PubMed: 8962159]

[19]. Wenzel HJ, Cole TB, Born DE, Schwartzkroin PA, Palmiter PD. Ultrastructural localization of zinc transporter-3 (ZnT-3) to synaptic vesicle membranes within mossy fiber boutons in the hippocampus of mouse and monkey. Proc. Natl. Acad. Sci. U. S. A 1997;94:12676–12681. [PubMed: 9356509]

[20]. Sindreu CB, Varoqui H, Erickson JD, Pérez-Clausell J. Boutons containing vesicular zinc define a subpopulation of synapses with low AMPAR content in rat hippocampus. Cerebral Cortex 2003;13:823–829. [PubMed: 12853368]

[21]. Cole TB, Wenzel HJ, Kafer KE, Schwartzkroin PA, Palmiter RD. Elimination of zinc from synaptic vesicles in the intact mouse brain by disruption of the ZnT3 gene. Proc. Natl. Acad. Sci. U. S. A 1999;96:1716–1721. [PubMed: 9990090]

[22]. Huang L, Gitschier J. A novel gene involved in zinc transport is deficient in the lethal milk mouse. Nat. Genet 1997;17:292–297. [PubMed: 9354792]

[23]. Liuzzi JP, Blanchard RK, Cousins RJ. Differential regulation of zinc transporter 1, 2, and 4 mRNA expression by dietary zinc in rats. J. Nutr 2001;131:46–52. [PubMed: 11208937]

[24]. Murgia C, Vespignani I, Cerase J, Nobili F, Perozzi G. Cloning, expression, and vesicular localization of zinc transporter Dri 27/ZnT4 in intestinal tissue and cells. Am. J. Physiol 1999;277:G1231–G1239. [PubMed: 10600821]

[25]. Huang L, Kirschke CP, Gitschier J. Functional characterization of a novel mammalian zinc transporter, ZnT6. J. Biol. Chem 2002;277:26389–26395. [PubMed: 11997387]

[26]. Kambe T, Narita H, Yamaguchi-Iwai Y, Hirose J, Amano T, Sugiura N, Sasaki R, Mori K, Iwanaga T, Nagao M. Cloning and characterization of a novel mammalian zinc transporter, zinc transporter 5, abundantly expressed in pancreatic beta cells. J. Biol. Chem 2002;24:19049–19055. [PubMed: 11904301]

[27]. Inoue K, Matsuda K, Itoh M, Kawaguchi H, Tomoike H, Aoyagi T, Nagai R, Hori M, Nakamura Y, Tanaka T. Osteopenia and male-specific sudden cardiac death in mice lacking a zinc transporter gene, ZnT5. Hum. Mol. Genet 2002;11:1775–1784. [PubMed: 12095919]

[28]. Kirschke CP, Huang L. ZnT7, a novel mammalian zinc transporter, accumulates zinc in the Golgi apparatus. J. Biol. Chem 2003;278:4096–4102. [PubMed: 12446736]

[29]. Chimienti F, Devergnas S, Favier A, Seve M. Identification and cloning of a beta-cell-specific zinc transporter, ZnT-8, localized into insulin secretory granules. Diabetes 2004;53:2330–2337. [PubMed: 15331542]

[30]. Robinson MS, Bonifacino JS. Adaptor-related proteins. Curr. Opin. Cell Biol 2001;13:444–453. [PubMed: 11454451]

[31]. Dell'Angelica EC, Shotelersuk V, Aguilar RC, Gahl WA, Bonifacino JS. Altered trafficking of lysosomal proteins in Hermansky-Pudlak syndrome due to mutations in the β3A subunit of the AP-3 adaptor. Mol. Cell 1999;3:11–21. [PubMed: 10024875]

[32]. Feng L, Seymour AB, Jiang S, To A, Peden AA, Novak EK, Zhen L, Rusiniak ME, Eicher EM, Robinson MS, Gorin MB, Swank RT. The β3A subunit gene (*Ap3b1*) of the AP-3 adaptor complex is altered in the mouse hypopigmentation mutant *pearl*, a model for Hermansky-Pudlak syndrome and night blindness. Hum. Mol. Genet 1999;8:323–330. [PubMed: 9931340]

[33]. Yang W, Li C, Ward DM, Kaplan J, Mansour SL. Defective organellar membrane protein trafficking in *Ap3b1*-deficient cells. J. Cell Sci 2000;113:4077–4086. [PubMed: 11058094]

[34]. Kantheti P, Qiao X, Diaz ME, Peden AA, Meyer GE, Carskadon SL, Kapfhamer D, Sufalko D, Robinson MS, Noebels JL, Burmeister M. Mutation in AP-3 δ in the mocha mouse links endosomal transport to storage deficiency in platelets, melanosomes, and synaptic vesicles. Neuron 1998;21:111–122. [PubMed: 9697856]

[35]. Salazar G, Love R, Werner E, Doucette MM, Cheng S, Levey A, Faundez V. The zinc transporter ZnT3 interacts with AP-3 and it is preferentially targeted to a distinct synaptic vesicle subpopulation. Mol. Biol. Cell 2004;15:575–587. [PubMed: 14657250]

[36]. Seong E, Wainer BH, Hughes ED, Saunders TL, Burmeister M, Faundez V. Genetic analysis of the neuronal and ubiquitous AP-3 adaptor complexes reveals divergent functions in brain. Mol. Biol. Cell 2005;16:128–140. [PubMed: 15537701]

[37]. Falcón-Pérez JM, Starcevic M, Gautam R, Dell'Angelica EC. BLOC-1, a novel complex containing the pallidin and muted proteins involved in the biogenesis of melanosomes and platelet-dense granules. J. Biol. Chem 2002;277:28191–28199. [PubMed: 12019270]

[38]. Martina JA, Moriyama K, Bonifacino JS. BLOC-3, a protein complex containing the Hermansky-Pudlak syndrome gene products HPS1 and HPS4. J. Biol. Chem 2003;278:29376–29384. [PubMed: 12756248]

[39]. Styers ML, Salazar G, Love R, Peden AA, Kowalczyk AP, Faundez V. The endo-lysosomal sorting machinery interacts with the intermediate filament cytoskeleton. Mol. Biol. Cell 2004;15:5369–5382. [PubMed: 15456899]

[40]. Kobayashi T, Beuchat MH, Lindsay M, Frias S, Palmiter RD, Sakuraba H, Parton RG, Gruenberg J. Late endosomal membranes rich in lysobisphosphatidic acid regulate cholesterol transport. Nat. Cell Biol 1999;1:113–118. [PubMed: 10559883]

[41]. Dell'Angelica EC, Ohno H, Ooi CE, Rabinovich E, Roche KW, Bonifacino JS. AP-3: an adaptor-like protein complex with ubiquitous expression. EMBO J 1997;16:917–928. [PubMed: 9118953]

[42]. Dell'Angelica EC, Aguilar RC, Wolins N, Hazelwood S, Gahl WA, Bonifacino JS. Molecular characterization of the protein encoded by the Hermansky-Pudlak syndrome type 1 gene. J. Biol. Chem 2000;275:1300–1306. [PubMed: 10625677]

[43]. Dell'Angelica EC, Ooi CE, Bonifacino JS. β3A-adaptin, a subunit of the adaptor-like complex AP-3. J. Biol. Chem 1997;272:15078–15084. [PubMed: 9182526]

[44]. Haase H, Beyersmann D. Intracellular zinc distribution and transport in C6 rat glioma cells. Biochem. Biophys. Res. Commun 2002;296:923–928. [PubMed: 12200136]

[45]. Ranaldi G, Perozzi G, Truong-Tran A, Zalewski PD, Murgia C. Intracellular distribution of labile Zn(II) and zinc transporter expression in kidney and MDCK cells. Am. J. Physiol. Renal Physiol 2002;283:F1365–F1375. [PubMed: 12388418]

[46]. Salazar G, Love R, Styers ML, Werner E, Peden A, Rodriguez S, Gearing M, Wainer BH, Faundez V. AP-3-dependent mechanisms control the targeting of a chloride channel (ClC-3) in neuronal and non-neuronal cells. J. Biol. Chem 2004;279:25430–25439. [PubMed: 15073168]

[47]. Salazar G, Craige B, Love R, Kalman D, Faundez V. Vglut1 and Znt3 cotargeting mechanisms regulate vesicular zinc stores in PC12 cells. J. Cell Sci 2005;118:1911–1921. [PubMed: 15860731]

[48]. Di Pietro SM, Falcón-Pérez JM, Tenza D, Setty SRG, Marks MS, Raposo G, Dell'Angelica EC. BLOC-1 interacts with BLOC-2 and AP-3 to facilitate protein trafficking on endosomes. Mol. Biol. Cell 2006;17:4027–4038. [PubMed: 16837549]

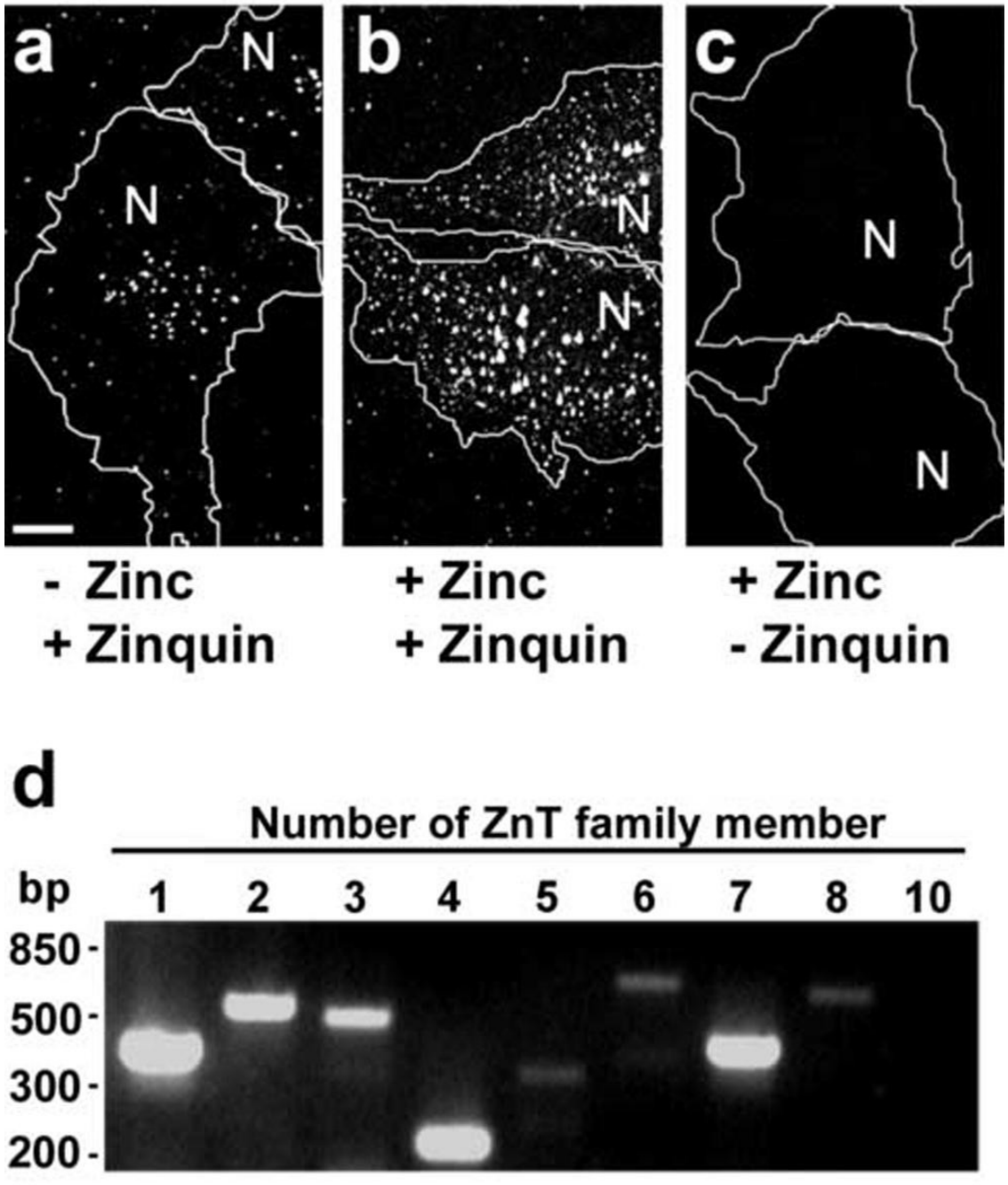

Fig 1.

Detection of intracellular stores of chelatable zinc and expression of ZnT family members in human M1 fibroblasts. (a-c) M1 fibroblasts were grown on monolayers and incubated in the absence (a) or presence (b,c) of 50 μM $ZnSO_4$, loaded with zinquin (a,b) or mock-loaded (c), and then fixed and analyzed by two-photon laser scanning microscopy. The approximate positions of the nucleus and limits of each cell are indicated with "N" and white lines, respectively. *Bar*, 10 μm. (d) Total RNA from M1 fibroblasts was extracted and subjected to RT-PCR using specific primers designed to detect expression of ZnT1 through ZnT8 and ZnT10, as indicated. The RT-PCR products were analyzed by 2.5% (w/v) agarose

electrophoresis in the presence of ethidium bromide. The approximate positions of molecular size standards are indicated on the left.

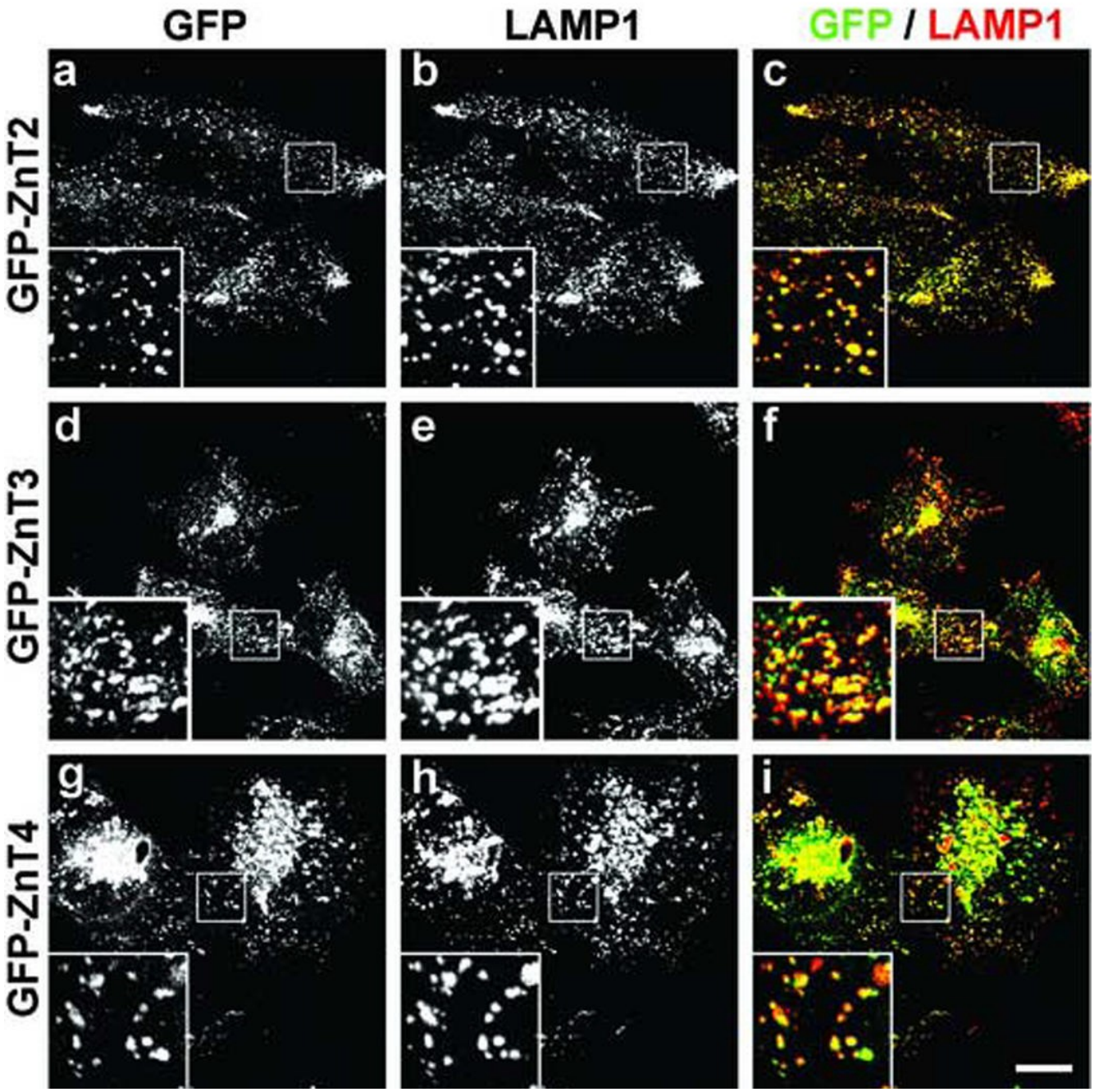

Fig 2.

Localization of GFP-tagged ZnT2, ZnT3 and ZnT4 proteins to late endocytic organelles of stably transfected M1 fibroblasts. (a-i) Stable M1 fibroblast lines expressing human ZnT2 (a-c), ZnT3 (d-f) or ZnT4 (g-i) fused at their N-terminus to GFP were subjected to immunostaining using a mouse monoclonal antibody against the late endosomal and lysosomal marker membrane protein, LAMP1, followed by Cy3-conjugated donkey anti-mouse IgG. Section images of GFP (a,d,g and green in c,f,i) and Cy3 (b,e,h and red in c,f,i) fluorescence were acquired on a two-photon confocal microscope using identical imaging conditions for all samples. The insets contain 3X-magnified views of selected areas indicated with *squares*. *Bar*, 20 μm.

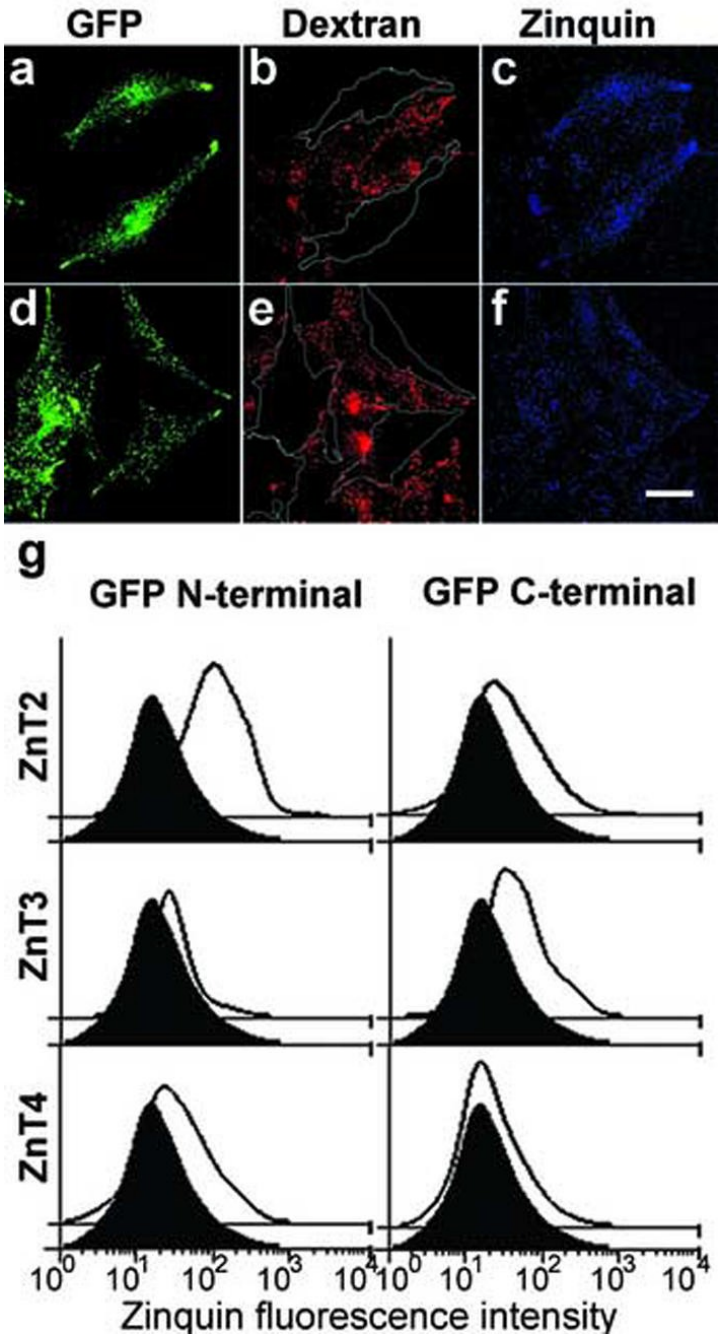

Fig 3.

Effects of the expression of GFP-tagged ZnT2, ZnT3 and ZnT4 proteins on the accumulation of chelatable zinc by human M1 fibroblasts. (a-f) Stable M1 fibroblasts expressing ZnT2 tagged with GFP at its aminoterminus (a-c) or at its carboxyl-terminus (d-f) were mixed and co-cultured with cells of the parental M1 line that had been previously loaded with Texas-red-conjugated dextran. Subsequently, cells were incubated with $ZnSO_4$, loaded with zinquin, and then fixed and analyzed by two-photon laser scanning microscopy. Each pair of GFP (a,d), Texas-red (b,e) and zinc-loaded zinquin (c,f) fluorescence images was acquired and processed under identical conditions. In (b and e), the approximate limits of ZnT2-positive cells are indicated with white lines. Note the increased zinquin fluorescence intensity in cells expressing

GFP-ZnT2, but not Znt2-GFP, as compared to the Texas-red-positive cells of the parental M1 line. *Bar*, 20 μm. (g) Flow cytometric analysis. Stable M1 fibroblasts expressing GFP-tagged ZnT2, ZnT3 or ZnT4 proteins (solid lines with no filling) or an unrelated GFP-tagged membrane protein (black filled curves) were incubated in presence of $ZnSO_4$, loaded with zinquin, and analyzed by flow cytometry. Shown are the distributions of zinquin fluorescence corresponding to at least 3,500 cells per sample; these cells were deemed to express comparable levels of each GFP-fusion protein as they were selected using an identical "gate" of GFP fluorescence intensity values (not shown).

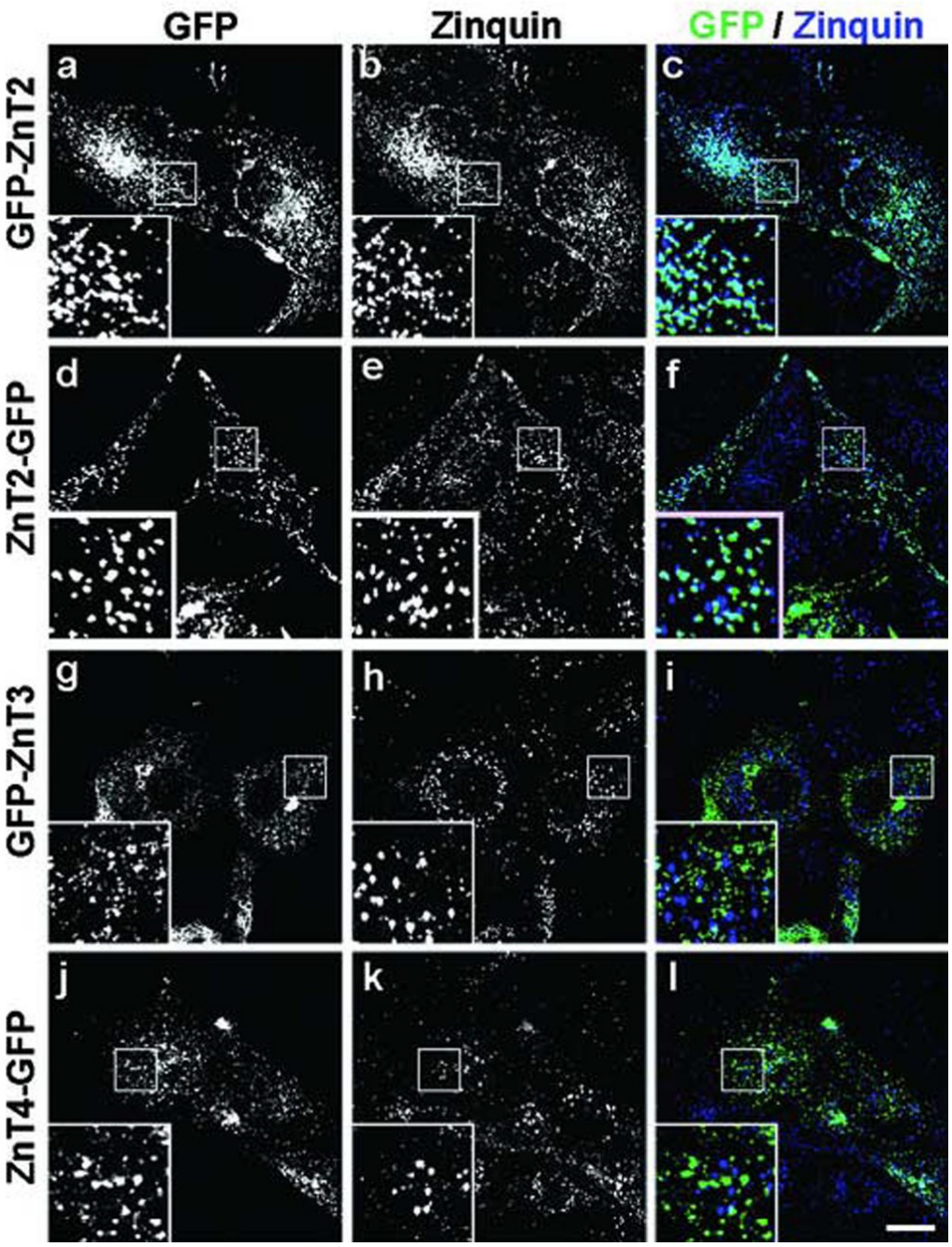

Fig 4.

Analysis of the colocalization of GFP-tagged ZnT2, ZnT3 and ZnT4 proteins with chelatable zinc stores in M1 cells. (a-l) Human M1 fibroblasts stably expressing ZnT2, ZnT3 or ZnT4 GFP-tagged at the N-terminus (GFP-ZnT2 and GFP-ZnT3) or C-terminus (ZnT2-GFP and ZnT4-GFP) were grown on glass coverslips, sequentially incubated with $ZnSO_4$ and zinquin, and then fixed and processed for two-photon laser scanning microscopy. Section images of GFP (a,d,g,j and green in c,f,i,l) and zinquin (b,e,h,k and blue in c,f,i,l) fluorescence were acquired using identical conditions for all samples. Magnified views (3X) of selected areas are shown in the insets. *Bar*, 20 μm.

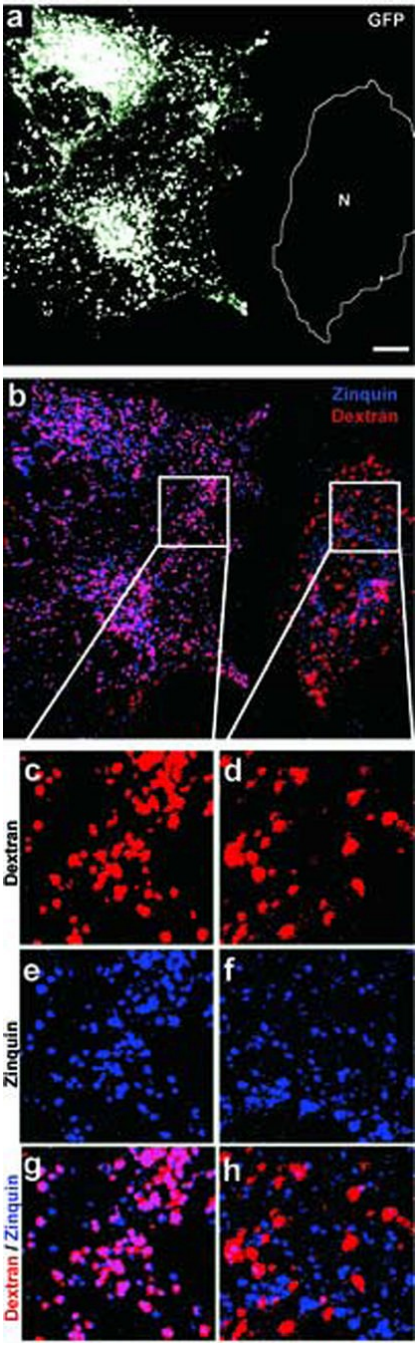

Fig 5.

Overexpression of GFP-ZnT2 elicits a shift in the distribution of chelatable zinc to mature lysosomes. (a-h) M1 fibroblasts were transiently transfected with a plasmid encoding the GFP-ZnT2 fusion protein, loaded with Texas-Red-conjugated dextran to label mature lysosomes, sequentially incubated with $ZnSO_4$ and zinquin, and then fixed and analyzed by two-photon laser scanning microscopy. Shown are representative images of GFP (a), Texas-Red (red in b,c,d,g,h) and zinquin (blue in b,e,f,g,h) fluorescence. The approximate position in (a) of a cell not expressing GFP-ZnT2 is denoted using "N" delimited by a white line. Magnified views of selected areas in cells expressing GFP-ZnT2 (c,e,g) or not transfected (d,f,h) are shown. Note the significant colocalization between the Texas-Red and zinquin fluorescence signals

observed in GFP-ZnT2-expressing cells and the poor overlap between these two fluorescence signals in control cells. *Bar*, 20 μm.

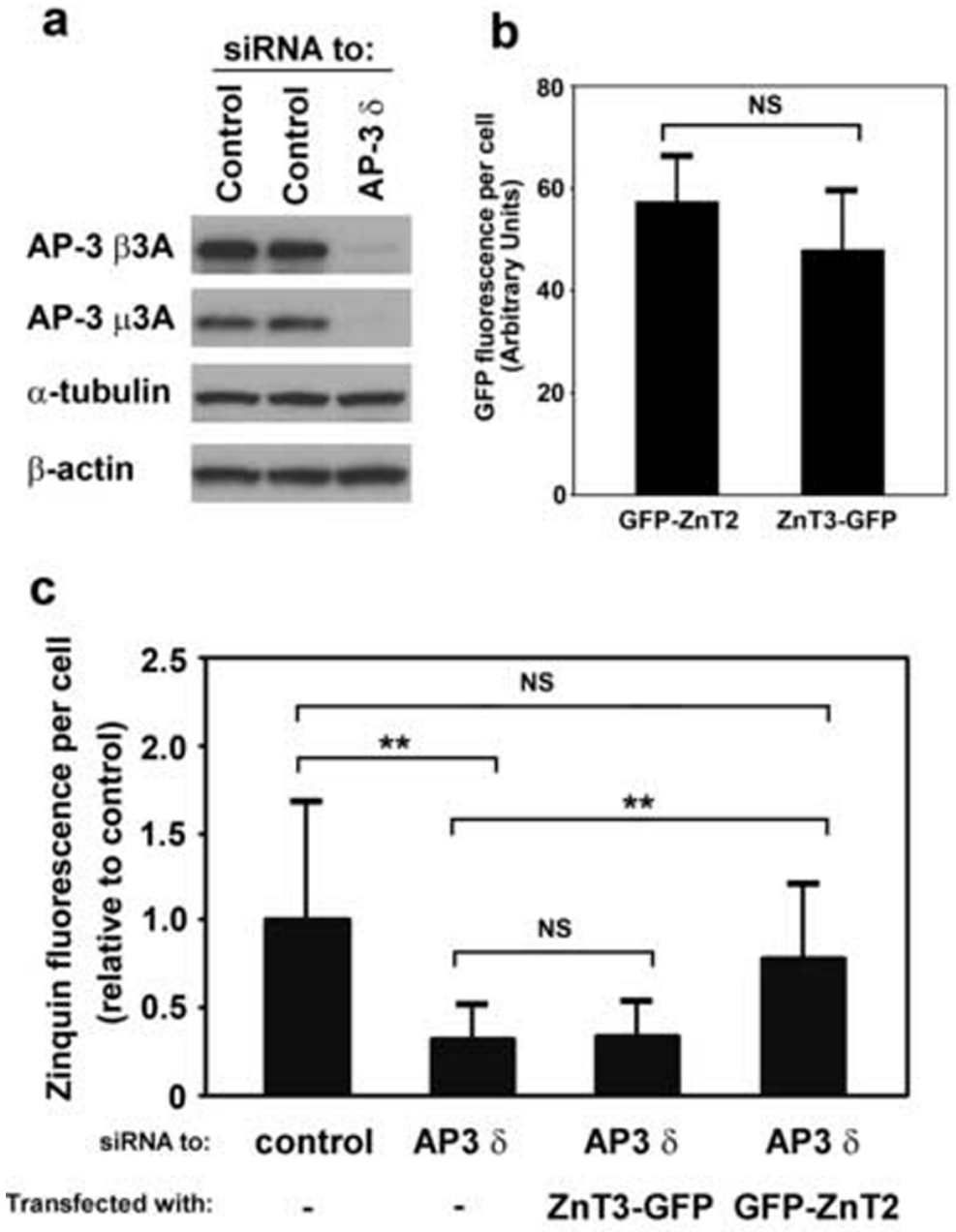

Fig 6.

Overexpression of GFP-tagged ZnT2 restores chelatable zinc stores in AP-3-depleted cells. (a-c) Cultured M1 fibroblasts were treated with control siRNA or with a siRNA duplex specifically designed to target the δ subunit of the AP-3 protein complex. (a) Whole-cell lysates were obtained and analyzed by immunoblotting, using antibodies against theβ3A and μ3A subunits of AP-3 as well as toα-tubulin andβ-actin. (b,c) M1 cells treated with siRNA were transiently transfected to overexpress GFP-ZnT2 or Znt3-GFP, and 24 h later they were sequentially incubated with $ZnSO_4$ and zinquin and analyzed by two-photon laser scanning microscopy. (b) GFP fluorescence levels in cells treated with siRNA specific to AP-3 δ and expressing either GFP-Znt2 or Znt3-GFP. Bars represent means ± SEM of values expressed

in arbitrary units. NS, not significant (Student's *t*-test). (c) Quantitative analysis of the levels of zinquin fluorescence observed in M1 fibroblasts treated with a control siRNA or with siRNA specific to AP-3 δ, and transiently transfected to overexpress GFP-tagged ZnT2 or ZnT3. The levels of zinquin fluorescence per cell were estimated by image analysis of 7-80 randomly selected cells per sample, and expressed as means ± SEM of the values normalized to the average zinquin fluorescence intensity of control cells. Kruskal-Wallis test followed by Dunn's multiple comparison test: NS, not significant; ** $p < 0.01$.

Table 1

Expression profile and subcellular distribution of ZnT family members in selected human cell lines

Family member	Expression of transcript[a]			Consensus subcellular distribution (M1 cells)[b]
	M1	HeLa	MNT-1	
ZnT1	+	+	+	Plasma membrane
ZnT2	+	+	ND[c]	Cytoplasmic foci
ZnT3	+	+	+	Cytoplasmic foci
ZnT4	+	+	+	Cytoplasmic foci
ZnT5	+	+	+	Golgi apparatus
ZnT6	+	+	+	Golgi apparatus
ZnT7	+	+	+	Golgi + cytoplasmic foci
ZnT8	+	ND	ND	ND
ZnT10	-	+	ND	ND

[a] As detected by RT-PCR. Human cell lines: M1 (fibroblastoid cell line), HeLa (cervix carcinoma cell line), MNT-1 (pigmented melanoma cell line).

[b] Subcellular distributions observed by fluorescence microscopy of M1 cells expressing each ZnT family member tagged with GFP at either the C- or N-terminus, as well as by indirect immunofluorescence staining of M1 cells expressing ZnT family members tagged with the myc epitope at the N-terminus.

[c] ND, not determined.